Stochastic model of stage transformation in graphite intercalation compounds

Hiroshi Miyazaki, Takeshi Watanabe, and Chuji Horie
Department of Applied Physics, Tohoku University, Sendai 980, Japan
(Received 11 April 1986)

A stochastic model is presented for stage transformation in graphite intercalation compounds. By introducing three types of intercalation processes into the domain model of Daumas and Hérold, we derive a nonlinear Langevin equation which describes the stochastic motion of intercalant islands. Results of simulation of the Langevin equation show that the stage transformation proceeds via initial nucleation of new stage regions followed by their growth. When the chemical potential of intercalants in the final state, μ_f, is taken in a certain range in the phase diagram, the time evolution of the structure factor demonstrates the coexistence and no significant broadening of peaks corresponding to the initial and final stage structures, in good agreement with experimental results. For other values of μ_f, the system transforms to the final stable stage via an intermediate disordered state or stays in a mixed state of stable stage and metastable stage. The appearance of metastable fractional stage units in the final state of the transformation is discussed.

I. INTRODUCTION

Graphite intercalation compounds (GIC's) are formed by the insertion of atomic or molecular layers of a different chemical species called the intercalant between layers in a host graphite material.[1] The intercalant layers in the ordered state of these compounds are arranged periodically along the c axis in the matrix of graphite layers. Thus, GIC's are classified by the stage number n denoting the number of carbon layers sandwiched between adjacent intercalant layers. This staging phenomenon characterized by the formation of ordered sequence of the host and intercalant layers and the staging transition associated with a change of stage number n are undoubtedly one of the most intriguing properties of GIC's and have been the subject of active studies over the past few years.

Although most of the experimental and theoretical work have been developed to investigate the equilibrium properties of staging phenomena, e.g., phase diagrams for staging, stage disorder, and staging transitions, some aspects of the kinetics of staging phenomena have been explored as well. An important detail of the staging transition is that it is considered to proceed by the formation and migration of islands of intercalants as was first proposed by Daumas and Hérold.[2] A physical rationale for the inhomogeneous distribution of intercalants was first suggested by Safran[3] based on the theory of spinodal decomposition. Later, Hawrylak and Subbaswamy[4] have investigated the kinetics of intercalation and staging transition using the time-dependent Landau-Ginzburg approach and have concluded that the formation of intercalant islands is a natural consequence of the kinetic constraint imposed by the intercalation mechanism. More detailed study of staging transition by taking account of the stacking entropy of intercalant layers has been carried out by Kirczenow,[5] in which it is suggested that the staging transitions proceed via stage-disordered states. This prediction seems to be qualitatively consistent with recent experiments by Misenheimer and Zabel[6] in which it was shown that high-stage K-GIC with $n \geqq 2$ exhibits, in thermal equilibrium, stage mixing and that the staging transitions from stage 5 to stage 4 and from stage 4 to stage 3 involve disordered states characterized by a broadening of the Bragg reflection.

Of greater interest, however, are recent experimental studies on the nonequilibrium properties in stage transformation which occur when GIC's are subject to a sudden change of vapor pressure of intercalants or temperature of specimen. Nishitani *et al.*[7] have performed *in situ* x-ray diffraction measurements of the isothermal stage transformation from stage 3 to stage 2 in K-GIC after a sudden change of vapor pressure of intercalants while the temperature of GIC is kept constant, and have obtained the result that the diffraction pattern corresponding to stage 2 grows gradually at the expense of the stage-3 pattern without showing any evidence for stage disorder. Similar results have been obtained by Misenheimer and Zabel[8] in the *in situ* observation of isobaric stage transformation from stage 1 to stage 2 in K-GIC after a sudden change of temperature of GIC in which the vapor pressure of intercalants is kept constant. It seems that the differences in the degree of stage disorder described in the above are not completely understood in terms of any theoretical model published so far. It is interesting, therefore, to study the nonequilibrium processes of stage transformation in order to see if the stage disorder is brought about during the stage transformation. The study of kinetics of staging may also provide us with a more detailed picture of stage transformations and intercalation processes.

In the present paper, we focus ourselves on the nonequilibrium processes and present a stochastic model of stage transformation which is based on the domain model of Daumas and Hérold (DH model) and the expression of free energy similar to that developed by Safran[9] and others.[10] In our stochastic model, the stage transformation is brought about by a simultaneous lateral translation of a slanting array of intercalant islands, a simultaneous shunting motion of the nearest-neighbor islands in adja-

cent layers, and a growth or diminution of islands due to intercalation or deintercalation from the edges of specimen. By dividing the crystal into columns along the c axis and introducing the average density of intercalants in a gallery within a column as the order parameter, we derive a nonlinear Langevin equation which describes the stochastic motion of intercalant islands. Simulation of the Langevin equation yields a snapshot of the motion of islands and, correspondingly, the time evolution of the x-ray structure factor, in the isothermal stage transformation from stage 3 to stage 2 after a sudden change of chemical potential or, equivalently, the vapor pressure of intercalants, our computer simulation shows that two well-ordered stages coexist during the transformation with no evidence for stage disorder. In agreement with experiment by Nishitani *et al.* Similar results are obtained for the case of isobaric transformation from stage 1 to stage 2 after a sudden change of temperature of GIC, which are also in qualitative agreement with experiment. It is to be noticed that those transformations accompanying no stage disorder can be realized only for cases where the final values of chemical potential or temperature fall in a certain range of values in the phase diagram.

A variety of cases of transformations realized within the present model are simulated by varying values of chemical potential of intercalants, temperature of GIC, and relevant parameters. For the case of stage transformation from stage 3 to stage 2 after a sudden change of temperature of GIC, but with constant chemical potential, it is found that the transformation proceeds via an intermediate disordered state in contrast to the results described above. It is also found that lowering the temperature of GIC makes intercalation processes slower and produces an intermediate state composed of stage-2 and stage-3 regions without showing tendency to approach a stable pure stage state. Discussion is made on the case when a fractional stage state appears in the course of stage transformation.

The outline of the present paper is as follows. In Sec. II, we describe our stochastic model of stage transformation. We give the expression of free energy of the present system and derive the nonlinear Langevin equation. In Sec. III, equilibrium phase diagram is determined from the free energy of the system and discussion is made concerning the appearance of fractional stages in the phase diagram. Simulating the Langevin equation, we present the results of time evolution of stage transformation in Sec. IV and compare them with experimental results. Section V is the conclusion with a discussion of the results.

II. STOCHASTIC MODEL OF STAGE TRANSFORMATION

An important detail of the mechanism of staging proposed by Daumas and Hérold[2] is that the intercalation proceeds by the formation of islands of intercalants in such a way that intercalants are distributed inhomogeneously between every pair of contiguous graphite layers. Inhomogeneous distribution of intercalants causes the elastic deformation of the host graphite layers.[11] This elastic deformation of graphite layers not only contributes to the cohesion of intercalants, i.e., the formation of intercalant islands, but also gives rise to the attractive interplanar interaction between islands for certain oblique directions.[10] Thus, the staggered juxtaposition of intercalant islands, in which the nearest-neighbor islands in adjacent gallaries occupy a staggered position in an oblique direction, is stabilized by the attractive interplanar interaction due to the elastic deformation of graphite layers. Figure 1(a) shows an example of staggered arrays of islands representing the stage-3 DH domain structure. According to the DH domain model, then, the stage transformation proceeds by the redistribution of intercalant islands inside the host graphite without the need for gross interdiffusion of intercalants between different layers.

In the present paper, we introduce in the DH domain model three types of intercalation processes for the stage transformation. The first is a simultaneous lateral translation of a slanting array of islands shown in Fig. 1(a). Since the slanting array of islands is stabilized by the attractive interaction between islands in an oblique direction, islands in an array tend to move simultaneously rather than separately. This simultaneous lateral translation of islands is driven by a successive intercalation or deintercalation from the edges of a sample. Thus, in the stage transformation from stage 3 to stage 2, slanting arrays are pushed inwards and the stage-2 regions grow inside the sample as shown in Fig. 1(a).

In Fig. 1(b) we show another example of stage-3 DH domain structure which gives the same structure factor $S(q_{\|})$ with $q_{\|}$ parallel to the c axis as that in Fig. 1(a). It is to be noticed that such an initial configuration of islands as shown in Fig. 1(b) cannot be transformed into a

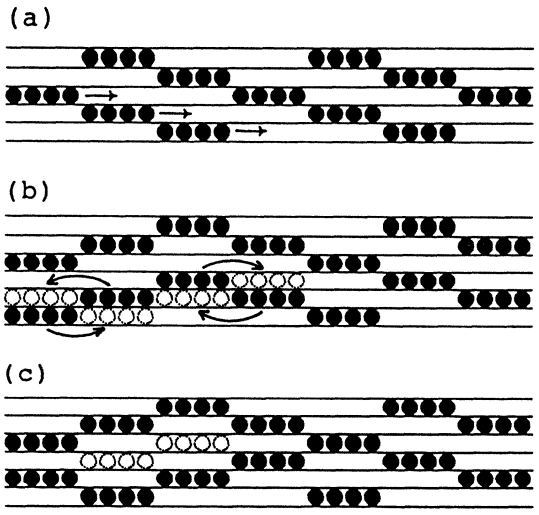

FIG. 1. Three types of intercalation processes are introduced in the present model. (a) Daumas-Hérold domain model for stage-3 structure. Arrows indicate a simultaneous lateral translation of a slanting array of islands. (b) Simultaneous shunting motion of islands shown by the arrows and dotted circles. (c) Growth process of islands shown by dotted circles, which produces two neighboring stage-2 units from the stage-4 unit.

stage-2 structure only by means of simultaneous lateral translations of islands. Therefore, we introduce the second type of intercalation process which is shown in Fig. 1(b), in which nearest-neighbor islands in adjacent layers move to their mirror position by means of mutual rotation. This simultaneous shunting motion of islands transforms two adjacent stage-3 units into stage-2 and stage-4 units. To recover the regular array we have to introduce the third type of intercalation process, which is a growth or diminution of islands in an empty interlayer space resulting from the diffusion of intercalants. This intercalation process produces two adjacent stage-2 units from the stage-4 unit as shown in Fig. 1(c).

For simplicity of discussion, we assume that the size of intercalant islands is almost equal to each other and remains unchanged even during the stage transformation. We divide the crystal into a set of columns along the c axis. Each column is subdivided into cells bounded by adjacent two-carbon layers. The size of the cell is taken to be large enough to accommodate only one intercalant island. Then, the well-ordered stage structure can be identified as a periodic occupation of cells by intercalant islands along the c axis. The mean density of intercalants in the nth cell of mth column, $\rho_{n,m}$, is taken as a stochastic variable which is defined by the number of intercalants $N_{n,m}$ in the cell divided by the number of sites N_0 available for the intercalants within the cell and is assumed to take a continuous value between 0 and 1.

In the following, we focus ourselves on the single column and describe the stage transformation in terms of a set of mean density of intercalants, ρ_n, in the nth cell within the single column. This model is called a single-column model. Within the framework of the single-column model, the simultaneous lateral translation and shunting motion of islands can be interpreted as an effective diffusion of intercalants along the c axis as shown in Fig. 1(b). Therefore, the stage transformation within the present model is brought about by an effective diffusion of intercalants along the c axis and a growth or diminution of islands within a cell of the column.

The free energy of a single-column model consists of two parts. One part is the intracolumn free energy Φ_1 first given by Safran,[9] and is written in terms of a set of mean density $\{\rho_n\}$ within a column as

$$\Phi_1 = -\tfrac{1}{2}U_0\sum_n \rho_n^2 + \tfrac{1}{2}\sum_{n,m} V_{n,m}\rho_n\rho_m + k_BT\sum_n [\rho_n \ln\rho_n + (1-\rho_n)\ln(1-\rho_n)] - \mu\sum_n \rho_n \ . \tag{2.1}$$

Here, the first term is the in-plane attractive interaction between intercalants ($U_0 > 0$) and contributes to the formation of islands. The second term represents the repulsive electrostatic interaction between ionized islands in the nth and mth cells along the c axis with $V_{n,m}$ given by

$$V_{n,m} = V_0 z_{n,m}^{-\alpha} \ , \tag{2.2}$$

where $z_{n,m}$ is the distance between cells n and m measured in units of the c-axis lattice spacing, and α is a positive parameter.[12] The third term in Eq. (2.1) is a mean-field entropy in the Bragg-Williams approximation, and μ in the last term represents the chemical potential of intercalants.

The other part of the free energy represents the intercolumn interaction originating from the elastic interaction between islands in different layers of different columns.[10,11] Elastic interaction is a long-range interaction and attractive between islands in different layers when islands are far apart. When they come close to each other and overlap along the c axis, the interaction becomes strongly repulsive. Therefore, the elastic interaction is responsible for the stabilization of staggered juxtaposition of islands. Stabilization of a juxtaposed configuration of islands can also be explained by considering the domain boundary energy of islands. Since the domain boundary energy is positive, the system tends to reduce its contribution to the total energy by letting the islands share common boundaries, resulting in the staggered configuration of islands shown in Figs. 1. Within the framework of the single-column model, the juxtaposed configuration of islands can be represented by the condition $\rho_n + \rho_{n+1} = 1$ in terms of a set of mean density $\{\rho_n\}$. In the present paper, therefore, we take into account the intercolumn interaction by adopting the expression

$$\Phi_2 = W_0 \sum_n [-2(\rho_n+\rho_{n+1})^2 + (\rho_n+\rho_{n+1})^4] \ . \tag{2.3}$$

It is seen that the intercolumn interaction Φ_2 takes a minimum energy $-W_0$ when the sum of intercalant densities in adjacent cells is equal to unity in correspondence to the most favorable configuration of islands.

Since the free energy within the framework of the single-column model is written in terms of mean density of intercalants in each cell $\{\rho_n\}$, we take $\{\rho_n\}$ as stochastic variables and derive a nonlinear Langevin equation which describes the stochastic motion of islands within a column. Details of its derivation are given in the Appendix,

$$\frac{d}{dt}\rho_n = -\sum_m \Delta_{n,m}\frac{\partial}{\partial\rho_m}\beta(\Phi_1+\Phi_2) + f_n(t) \ , \tag{2.4}$$

where $\Delta_{n,m}$ is a kinetic coefficient given by

$$\Delta_{n,m} = \begin{cases} 2A+B, & n=m \\ -A, & n=m\pm 1 \end{cases} \tag{2.5}$$

$\beta = 1/k_BT$, and $f_n(t)$ is the Gaussian-Markovian random forces satisfying the fluctuation-dissipation theorem,

$$\langle f_n(t) f_m(t')\rangle = 2\Delta_{n,m}\delta(t-t') \ . \tag{2.6}$$

In the expression of kinetic coefficients (2.5), A and B represent the effective diffusion rate of intercalants along the c axis and the growth or diminution rate of islands within a cell, respectively. It is to be noted that if we take the total number of intercalants within a column as the order parameter, the effective diffusion process conserves the order parameter, while the growth or diminution process does not conserve it. Therefore, the present system is not only nonlinear in a sense that its time evolution is governed by a nonlinear Langevin equation, but also

represents the most general case of phase transformation including both conserving and nonconserving processes of order parameters.

III. EQUILIBRIUM PHASE DIAGRAM

Before discussing the results of simulation, we give the equilibrium phase diagram of the present system and see what kind of role the intercolumn interaction Φ_2 plays to establish the equilibrium state of the system. The equilibrium phase diagram is determined by minimizing the free energy $\Phi_1+\Phi_2$ with respect to a set of mean density $\{\rho_n\}$. Figure 2 shows an example of the equilibrium phase diagram as a function of temperature of GIC, T_G, and chemical potential for intercalants, μ. Here, the values of relevant parameters are taken in units of in-plane attractive interaction U_0 as $V_0=0.2$ and $\alpha=3$ for repulsive electrostatic interaction and $W_0=0.02$ for intercolumn interaction. In describing various phases which appear in the phase diagram, we use the term "stage-(n/m) phase" to mean a periodic structure consisting of n cells m of which are occupied by the intercalant islands. Stage n (case of $m=1$) refers to the pure stage which has been observed experimentally. All the stages (n/m) with $m\neq 1$ are called fractional stages.

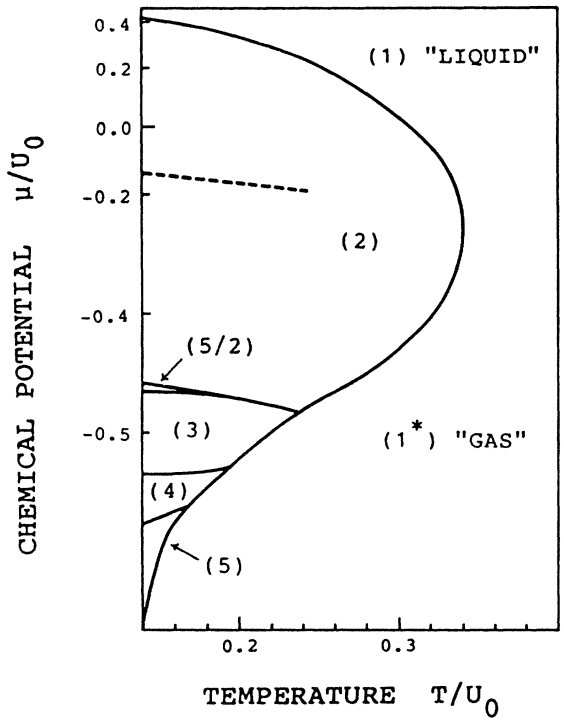

FIG. 2. Equilibrium phase diagram for $V_0=0.2U_0$, $\alpha=3$, and $W_0=0.02U_0$ plotted as a function of temperature T_G and chemical potential μ, both normalized to U_0. Integers and fraction, $\frac{5}{2}$, in parentheses are the stable stage phases within the maximum stage number to be 5. Dashed line in the stage-2 phase represents the chemical potential μ^* which is concerned with metastable stage-3 and stage-$\frac{3}{2}$ states as is described in the text.

In the determination of phase diagram shown in Fig. 2, we restrict the number of stage to be less than 6 and compare free energy of every configuration of islands within this restriction including not only the pure stage structures but also the fractional stages of $\frac{3}{2}$, $\frac{5}{2}$, $\frac{4}{3}$, $\frac{5}{3}$, and $\frac{5}{4}$. Then, we found for adopted values of parameters that all the fractional stages except $\frac{5}{2}$ are either unstable or metastable and do not appear as an absolutely stable state in the phase diagram. The fractional stage-$\frac{5}{2}$ phase appearing in the phase diagram at low temperatures between stage-2 and stage-3 phases consists of an alternate stacking of stage-2- and stage-3-like units.

All the fractional stages except $\frac{5}{2}$ have a common feature that some of the adjacent cells in a repeat unit are simultaneously occupied by intercalant islands. For such a configuration of islands, the intercolumn interaction Φ_2 becomes strongly repulsive so that the fractional stages like $\frac{3}{2}$ ceases to be stable.

It should be noted that Millman and Kirczenow[13] have also obtained a phase diagram in which no fractional stage phases appear by adopting a strongly screened electrostatic interaction between islands:[14]

$$V_{n,m}=V_0 z_{n,m}^{-\alpha}\eta_{n,m}\ , \tag{3.1}$$

where $\eta_{n,m}=1$ if there is no intercalant islands between cells n and m and $\eta_{n,m}=0$ otherwise. In the present work, we take no account of this strong screening of the electrostatic interaction, since one of the purposes of the present paper is to investigate the role of the intercolumn interaction Φ_2 in the equilibrium as well as nonequilibrium properties of staging phenomena.

The dashed line in the stage-2 region of the phase diagram in Fig. 2 represents the chemical potential μ^* which is the boundary between the metastable stage-3 phase and fractional stage-$\frac{3}{2}$ phase. For a region of chemical potential higher than μ^*, the fractional stage-$\frac{3}{2}$ phase has lower free energy than the pure stage-3 phase, both of which, of course, have higher free energy than that of stage-2 phase. As will be discussed in Sec. IV, μ^* represents a critical value for the chemical potential concerning the appearance of metastable fractional stage units in the final equilibrium state of the stage transformation.

IV. TIME EVOLUTION OF STAGE TRANSFORMATION

Based on the discussion of equilibrium properties of the present system in Sec. III, we study the time evolution of stage transformation for a variety of cases by simulating the Langevin equation (2.4). In the simulation, the size of the system is taken to be 60 cells and the periodic boundary condition is imposed for the mean density of intercalants in each cell ρ_n. Numerical integration of the equation is carried out with the aid of Rung-Kutta method. After evaluating the systematic forces due to free energy of the system at each step of integration, we add to the right-hand side (rhs) of Eq. (2.4) random forces $\{f_n(t)\}$ generated in accordance with Eq. (2.6).[15] As for the magnitude of random forces, we have introduced a factor γ which reduces $f_n(t)$ to $\gamma f_n(t)$ at each cell. We

found in the simulation that the density fluctuation of each cell in the case without the reduction factor γ becomes large so that it takes too long a time for the system to settle down to a new equilibrium state. The reason for the introduction of reduction factor γ is simply to shorten the computation time of simulation. In the following, we present the results of simulation for stage transformations from stage 3 to stage 2 and from stage 1 to stage 2, since we are particularly interested in the experimental results described in Sec. I.

A. Isothermal stage transformation from stage 3 to stage 2 after a sudden change of μ

As an example of isothermal stage transformation, we consider the case of transformation from stage 3 to stage 2 after a sudden change of the chemical potential from $\mu=-0.5$ at which the system is in equilibrium pure stage 3 to $\mu=-0.16$ which corresponds to stage 2. Here, in-plane attractive interaction U_0 is taken as the units of energy which was estimated to be about 2400 K in Cs-GIC by Safran.[9] During the transformation, temperature of GIC, T_G, is kept constant at $T_G=0.2$. Other values of parameters are as follows: $V_0=0.2$ and $\alpha=3$ for electrostatic interaction. $W_0=0.02$ for intercolumn interaction, $A=3.0$ and $B=15.0$ for effective diffusion rate and growth rate, respectively, and $\gamma=0.01$ for the reduction factor of random forces.

An interesting point of the present simulation is that we can directly observe the snapshot of density profile $\{\rho_n(t)\}$ of the system during the stage transformation as shown in Fig. 3. From the figure, we can see that the stage transformation begins with a local change of two adjacent stage-3 units into three stage-2 units. Then, the nucleated stage-2 region grows in size, producing a large well-ordered region of stage 2. This growth process of the stage-2 region can be interpreted as the propagation of boundaries between well-ordered stage-2 and stage-3 regions. The well-ordered stage-2 region grows up further by the collision with other stage-2 regions accompanying the vanishment of boundaries. There are cases when the collision of the boundaries leaves a metastable stage-3 unit behind, since the initial nucleation of stage-2 units takes place at random by the random forces. Remaining metastable stage-3 units bring about in the structure factor the broadening of the peak which corresponds to the well-ordered stage-2 structure.

From the values of mean density $\{\rho_n(t)\}$ at each step of simulation, we can evaluate the structure factor $S(q,t)$ defined by

$$S(q,t)=\frac{1}{N}\sum_{n,m}\langle\rho_n(t)\rho_m(t)\rangle\exp[-iq(n-m)c]\ , \qquad (4.1)$$

where N is the total number of cells within a column and c is the thickness of each cell. Here, the thickness of the cell c is assumed to be constant during the stage transformation for simplicity of calculation, which does not change the qualitative conclusion of the present study. The notation $\langle\cdots\rangle$ means the ensemble average. Figure 4 shows the time evolution of structure factor $S(q,t)$ averaged over ten runs of simulation. Sharp peaks at $q=2\pi/3c$ and $q=\pi/c$ correspond, respectively, to the initial stage-3 and final stage-2 structures. It is interesting to observe from the figure that the stage-2 peak grows gradually at the expense of the initial stage-3 peak and that both peaks coexist in the course of stage transformation without any significant broadening of peaks. These results are in good agreement with the results of *in situ* isothermal experiment[7] and supports a simple picture of stage transformation that stage transformation proceeds via a propagation of boundaries between well-ordered stage regions. From the width of the stage-2 peak, the correlation length along the c axis of the final stage-2

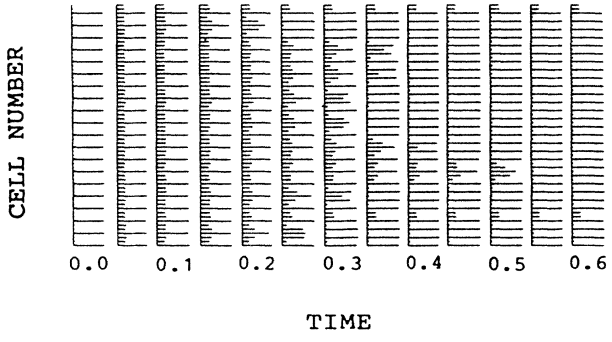

FIG. 3. Time evolution of density profile $\{\rho_n(t)\}$ in the isothermal stage transformation from stage 3 to stage 2. Values of parameters are $T_G=0.2$, $V_0=0.2$, and $W_0=0.02$ in units of U_0 and $\alpha=3$. Chemical potential is changed from $\mu=-0.5$ to $\mu=-0.16$. Kinetic coefficients, A and B, are taken as 3.0 and 15.0, respectively. Reduction factor γ for random forces is taken to be 0.01.

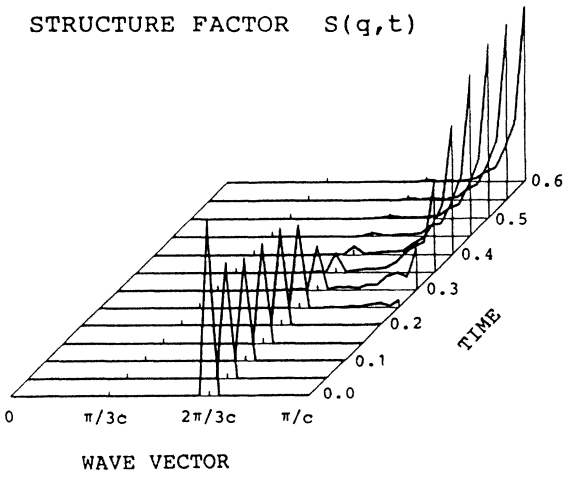

FIG. 4. Time evolution of structure factor $S(q,t)$ averaged over ten runs of simulation for the same values of parameters and change of chemical potential as in the case shown in Fig. 3. c is the thickness of cell. Plot of $S(q,t)$ at $q=0$ is omitted for clarity.

structure is estimated to be about 30 cells. It is confirmed that this correlation length is almost the same irrespective of the size of the system for the same values of parameters.

The value of chemical potential μ_f in the final equilibrium state has a significant influence on the time evolution of stage transformation. In the simulation described above, we have chosen the value of μ_f to be just below μ^* shown by the dashed line in the phase diagram in Fig. 2. When μ_f exceeds μ^*, the final state of the system generally contains fractional stage units instead of metastable stage-3 units as a consequence of the fact that for value of $\mu_f > \mu^*$ the metastable fractional stage state has lower free energy than the stage-3 state. For values of μ_f chosen to be in the vicinity of the phase boundary between stages 1 and 2, we observe that the system first transforms into stage-1 state and then to the final equilibrium stage-2 state, and the coexistence of stage-2 and stage-3 peaks in the structure factor becomes less noticeable.

In the opposite case of $\mu_f < \mu^*$, the intercalation process becomes slower for lower values of μ_f. Figure 5 shows the time evolution of structure factor for the case of $\mu_f = -0.2$ at constant temperature $T_G = 0.2$. We can see that the growth of the stage-2 peak becomes slower and the stage-2 peak finally becomes much broader than in the case of $\mu_f = -0.16$ shown in Fig. 4. This broadening of the stage-2 peak reflects the fact that the final state of the system consists of a mixture of well-ordered stage-2 regions and metastable stage-3 regions with the size extending from a minimum of 3 cells to an even 21 cells. Therefore, the lower value of μ_f is responsible for the appearance of an intermediate mixed state composed of stage-2 and stage-3 regions and eventually prevents the system from approaching the final equilibrium stage-2 state.

General features of the isothermal stage transformation in response to μ_f described above are not found to be significantly affected by the temperature of GIC, even though the transformation becomes slower at lower temperatures.

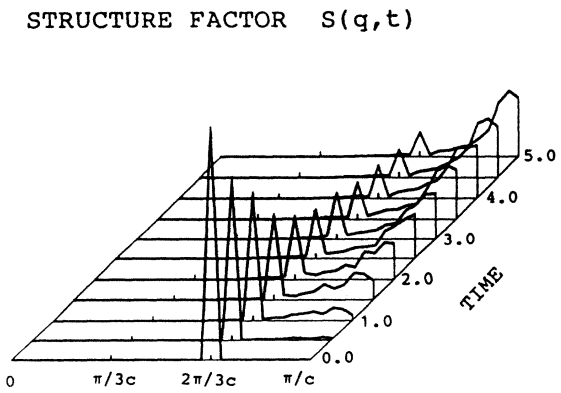

FIG. 5. Time evolution of structure factor $S(q,t)$ corresponding to the isothermal stage transformation from stage 3 to stage 2 at $T_G = 0.2$, where the chemical potential is changed from $\mu = -0.5$ to $\mu = -0.2$. Other values of parameters are the same as in the case shown in Fig. 3.

B. Stage transformation from stage 3 to stage 2 after a sudden change of T_G for constant μ

In contrast to the isothermal stage transformation, the results of stage transformation from stage 3 to stage 2 after a sudden change of temperature of GIC, T_G, for a constant value of chemical potential μ shows a remarkable difference in the time evolution of structure factor and density profile. In Fig. 6, we show the time evolution of structure factor $S(q,t)$ averaged over ten runs of simulation in which μ is kept constant at $\mu = -0.48$ and T_G is suddenly changed from $T_G = 0.14$ at which the system is in equilibrium pure stage 3 to $T_G = 0.245$ which corresponds to stage 2. Other values of parameters are the same as in the isothermal stage transformation shown in Figs. 3 and 4. The structure factor exhibits double peaks in the vicinity of $q = \pi/c$ in the intermediate state of simulation and the stage-2 peak in the final state remains broad in contrast to the case of isothermal transformation. The correlation length along the c axis of the final stage-2 state is about ten cells. Thus, the time evolution of structure factor indicates the presence of disorder in the course of stage transformation.

From the time evolution of density profile in the present case, it is found that the transformation proceeds via an intermediate state in which stage-1, stage-2, and stage-3 units are mixed up. Instead of initial local change from two adjacent stage-3 units to three stage-2 units, adjacent stage-3 units first become stage-1 regions and then the stage-2 structure grows gradually. This feature of transformation can be understood by the fact that we have chosen the final T_G in the vicinity of phase boundary between stage-1 and stage-2 states in the phase diagram. It is found that the feature of time evolution of the system is sensitive to the final value of T_G.

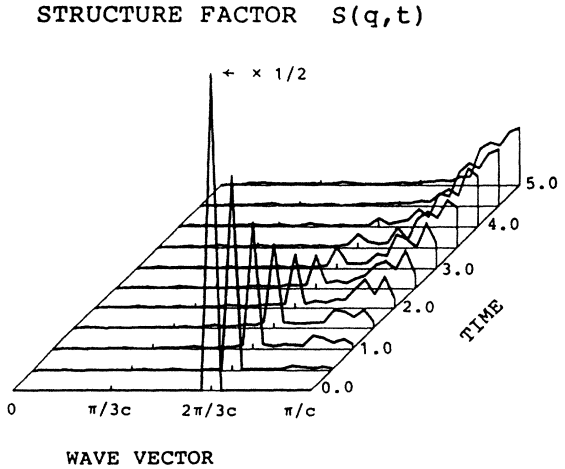

FIG. 6. Time evolution of structure factor $S(q,t)$ corresponding to the stage transformation from stage 3 to stage 2 in which temperature of GIC is suddenly changed from $T_G = 0.14$ to $T_G = 0.245$. Value of chemical potential is fixed as $\mu = 0.48$. Reduction factor γ for random force is chosen as $\gamma = 0.05$. Other values of parameters are the same as in the case shown in Fig. 3. Components of $S(q,t)$ at $t = 0$ are reduced to one-half for clarity.

C. Isobaric stage transformation from stage 3 to stage 2

In the isobaric stage transformation one changes the temperature of GIC T_G while keeping the vapor pressure of intercalants constant. Since the chemical potential μ of intercalants is given as a function of T_G as well as vapor pressure, a sudden change of T_G inevitably involves the change of chemical potential. In the isobaric transformation, therefore, both the values of T_G and μ are suddenly changed simultaneously. In order to see the difference of time evolution of isothermal and isobaric transformations from stage 3 to stage 2 we have performed simulations of stage transformation in which we vary the initial values of μ and T_G while fixing their final values as $\mu=-0.16$ and $T_G=0.2$. It is found that the final pattern of the structure factor is almost independent of the initial state of the system. However, the time evolution of stage transformation is found to be sensitive to the value of μ_f. This dependence on μ_f is qualitatively the same as that described in Sec. IV A. Within the present model, therefore, we observe almost no difference of the time evolution between the isothermal and isobaric transformations.

D. Stage transformation from stage 1 to stage 2

We have also carried out simulations of isobaric stage transformation from stage 1 to stage 2. In Fig. 7, we show a typical example of the time evolution of structure factor $S(q,t)$ averaged over ten runs of simulation. In the simulation, values of μ and T_G are initially taken as $\mu=0.4$ and $T_G=0.18$, at which point the system is in pure stage-1 state, and are suddenly changed to $\mu=0.0$ and $T_G=0.2$ corresponding to the stage-2 state. Other values of parameters are the same as in the case shown in Fig. 4. Peaks in the vicinity of $q=0$ and $q=\pi/c$ correspond to stage-1 and stage-2 structures, respectively. It is seen that the growth or diminution of these peaks is accompanied by no significant broadening, in agreement with the experimental results.[8] Time evolution of density profile again confirms a simple picture of stage transformation in that the transformation proceeds with an initial nucleation of stage-2 units followed by the growth of stage-2 regions.

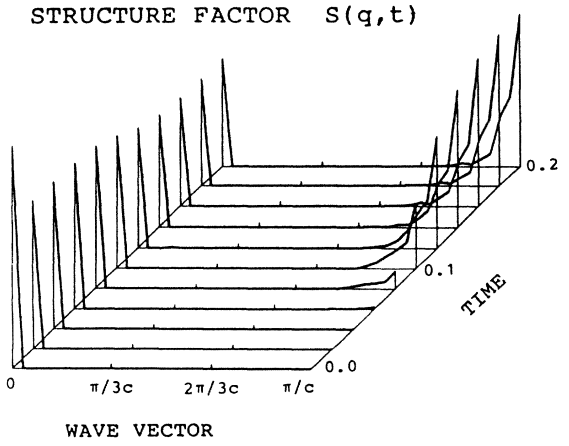

FIG. 7. Time evolution of structure factor $S(q,t)$ corresponding to the stage transformation from stage 1 to stage 2. In the simulation, values of chemical potential μ and temperature of GIC T_G are simultaneously changed as μ: $0.4\rightarrow0.0$, and T_G: $0.18\rightarrow0.2$. Components of $S(q,t)$ at $q=0$ are reduced to one-tenth.

The isothermal stage transformation from stage 1 to stage 2 for a sudden change of chemical potential was also simulated. Note that the simulation for the case of $\mu=0.4\rightarrow\mu=0.0$ at constant temperature $T_G=0.2$ gives the same pattern of structure factor as that shown in Fig. 7. The same pattern is also obtained for stage transformation for a sudden change of temperature from $T_G=0.31$ to $T_G=0.2$ at constant chemical potential $\mu=0.0$. These simulations confirm the fact that the stage transformation is insensitive to the initial state of the system as is the case for the stage transformation from stage 3 to stage 2 described in Sec. IV A.

V. DISCUSSION AND SUMMARY

As has been pointed out in Sec. IV A the time evolution of stage transformation depends sensitively on the final values of chemical potential and temperature of GIC. It also depends on the intercolumn interaction Φ_2 and kinetic coefficients, i.e., effective diffusion rate A along the c axis and growth rate B. In what follows we discuss the role of these parameters in the time evolution of the system, based on the results of simulation of the isothermal stage transformation.

The fact that the stage transformation becomes faster for higher values of μ_f seems to be associated with the decrease of potential barrier between initial stage-3 and final stage-2 states. However, since it is difficult to estimate the magnitude of the potential barrier, we describe the μ_f dependence of the transformation process in terms of the time evolution of density profile $\{\rho_l\}$. In response to a sudden increase of μ, the total density of intercalants increases in a way that the difference of density of each cell tends to diminish, and consequently it becomes easy to produce the final stage-2 state.

On the other hand, for lower values of μ_f, the transformation becomes slow and the system transforms into a mixed state consisting of stage-2 and metastable stage-3 regions. This tendency, of course, is entirely dependent of the fact that there exists a metastable state with free energy close to that of the absolutely stable state for chosen values of μ_f and T_G.

Let us discuss the role of intercolumn interaction Φ_2. In the case for μ_f just above μ^*, if the magnitude of Φ_2, i.e., W_0 is reduced to smaller values, e.g., 0.005, we observe that it takes too long a time for the system to begin the initial nucleation in response to the sudden change of μ. This is in contrast to the case for $W_0=0.02$ described in Sec. IV. For higher values of μ_f, the transformation towards the stage-2 state occurs more easily. However, the stage-2 peak of the structure factor in the final state becomes broader, and final density profile becomes a mixture of stage-2 and metastable fractional stage-$\frac{3}{2}$ units. From these results it is concluded that in the present model the intercolumn interaction Φ_2 plays an essential role in inducing the initial nucleation of stage-2 units and

in depressing the appearance of fractional stage units in the stage transformation from stage 3 to stage 2.

Next, we discuss the role of kinetic coefficients, i.e., the effective diffusion rate A along the c axis and the growth rate B, in the stage transformation. We have carried out simulations of stage transformation from stage 3 to stage 2 for extreme cases of $A \gg B$ and $A \ll B$. It is found that it takes longer time for the system to start the initial nucleation process for the case of $A \gg B$ than the case of $A \ll B$. We have also observed that larger value of B shortens the time for the system to reach the final equilibrium state but broadens the final stage-2 peak.

Since the stage transformation is necessarily accompanied by the change of the total number of intercalants within the sample, the growth process is expected to play an important role in the transformation. When the growth process dominates over the diffusion process, i.e., $A \ll B$, it is confirmed that the initial nucleation of stage-2 units takes place at the early stage of transformation. Besides, initial nucleation processes take place almost simultaneously with a short correlation length along the c axis so that the final stage-2 peak in the structure factor becomes broad. On the other hand, when the diffusion process dominates over the growth process, i.e., $A \gg B$, the system first transforms into a metastable stage-3 state and then there occurs the nucleation and growth of stage-2 region. The nucleation and growth of stage-2 region proceeds accompanying a long correlation along the c axis. Thus, the final stage-2 state in this case is well ordered and gives a sharp stage-2 peak in the structure factor.

It should be noted that the stage disorder found in the present simulation is a consequence of the kinetics of intercalation in accordance with the suggestion by Bak and Forgacs.[16] Although Kirczenow[5] has argued that the entropy due to the stacking disorder of intercalant islands is crucial in yielding static stage-disordered states, the term representing the entropy due to stacking disorder was not introduced in the present single-column model, because the existence of stage-disordered states was not assumed *a priori*. This result of the appearance of stage disorder, which is induced kinetically, is also consistent with the recent three-dimensional Monte Carlo simulation by Kirczenow.[17]

So far we have summarized the details of simulation for stage transformations from stage 3 to stage 2 and stage 1 to stage 2. Although the present single-column model seems to be suitable in describing those cases which involve the stage-2 state as a final state, it is not entirely appropriate to present the more general guideline on when stage order or disorder is to be expected for higher stages. In fact, while the intercolumn interaction Φ_2 is favorable in producing the stage-2 units during the stage transformation, it is not necessarily responsible for the appearance of the stage-3 units, for example. The same argument applies to the case of simulation of successive stage transformations.[18] We have simulated the stage transformations from stage 4 to stage 2 and from stage 5 to stage 2 for a sudden change of μ, but have found no indication of successive transformations, i.e., $4 \rightarrow 3 \rightarrow 2$ or $5 \rightarrow 4 \rightarrow 3 \rightarrow 2$. Therefore, it seems necessary to improve the present single-column model by taking into account a proper effect of intercolumn interaction which would be responsible for the initial nucleation of not only stage-2 but also stage-3 units. The details will be published in a separate paper.

These results of the present study of the time evolution of stage transformation are summarized as follows. (i) In the isothermal stage transformation from stage 3 to stage 2 after a sudden change of chemical potential to μ_f which is just below μ^* (cf. Fig. 2), well-ordered regions of stage-2 and stage-3 states coexist and the structure factor shows no significant broadening of peaks during the stage transformation. These features are in qualitative agreement with experimental results. The time evolution of density profile provides us with a simple picture of stage transformation that the stage transformation is initiated by the nucleation of stage-2 units due to the local change of stage-3 units into stage-2 units and then proceeds with the propagation of boundaries between well-ordered stage regions. (ii) This simple picture of stage transformation is found to be applicable to other cases of stage transformation from stage 1 to stage 2. Time evolution of the corresponding structure factor shows a growth of the sharp stage-2 peak in agreement with the results of isobaric experiments. (iii) In general, time evolution of the system is governed by the final values of chemical potential μ_f, but is almost independent of the initial state of the system. General features of the stage transformation seem to depend on how the metastable phases come close to the most stable phase in the final state. For higher values of μ_f beyond μ^*, the density profile of initial stage 3 changes to a pattern composed of well-ordered stage-2 regions separated either by the metastable stage-3 or fractional stage-$\frac{3}{2}$ units. It is also found that in some cases where $\mu_f < \mu^*$, the system transforms into intermediate states composed of randomly mixed stage-2 and stage-3 regions and eventually ceases to approach the absolutely stable pure stage-2 structure. (iv) Intercolumn interaction provides a potential barrier to the formation of fractional stage units and depresses the appearance of these units in the final state of the system. On the other hand, this interaction plays a role of promoting the initial nucleation of stage-2 units from the stage-3 region. (v) When the effective diffusion of intercalants along the c axis dominates over the growth of intercalants in each cell, the system transforms to a metastable stage-3 state and then to the final stage-2 state by the systematic nucleation and growth of stage-2 regions. This yields a sharp stage-2 peak in the final state of the structure factor. In the opposite case, the stage transformation becomes faster but the final structure factor shows a broad stage-2 peak.

ACKNOWLEDGMENTS

The authors wish to thank J. E. Fisher and S. A. Solin for fruitful discussions and comments. This work is supported by a Grant-in-Aid for Scientific Research from the Ministry of Education, Science and Culture, Japan.

APPENDIX

In this appendix we give the derivation of the Langevin equation (2.4). We start with a master equation of the distribution function $P(\{\rho_l\},t)$ for a set of mean densities $\{\rho_l\}$ of intercalants in each cell in the single column. Then, the Fokker-Planck equation is derived from the master equation. Finally, we construct the Langevin equation by introducing Gaussian-Markovian random forces, which is equivalent to the Fokker-Planck equation.

As has been described in the text, the simultaneous lateral translation and shunting motion of islands can be interpreted within the framework of a single-column model as an effective diffusion of intercalants along the c axis. In correspondence to this diffusion process, we introduce the transition probability $W_{nm}(\rho_n\to\rho_n+\Delta;\rho_m\to\rho_m-\Delta)$ which describes an exchange of intercalants by an amount Δ between nth and mth cells. We also define the growth rate $U_n(\rho_n\to\rho_n+\Delta)$ for the change of intercalant density at nth cell. Then, it is straightforward to write down the master equation for the distribution function $P(\{\rho_l\},t)$ which is equal to the probability that the system will be found in the configuration $\{\rho_l\}$ at time t,

$$\begin{aligned}\frac{\partial}{\partial t}P(\{\rho_l\},t)=&-\sum_{(n,m)}\sum_{\Delta}W_{nm}(\rho_n\to\rho_n-\Delta;\rho_m\to\rho_m+\Delta)P(\{\ldots,\rho_n,\ldots,\rho_m,\ldots\},t)\\&+\sum_{(n,m)}\sum_{\Delta}W_{nm}(\rho_n+\Delta\to\rho_n;\rho_m-\Delta\to\rho_m)P(\{\ldots,\rho_n+\Delta,\ldots,\rho_m-\Delta,\ldots\},t)\\&-\sum_{n}\sum_{\Delta}U_n(\rho_n\to\rho_n-\Delta)P(\{\ldots,\rho_n,\ldots\},t)\\&+\sum_{n}\sum_{\Delta}U_n(\rho_n+\Delta\to\rho_n)P(\{\ldots,\rho_n+\Delta,\ldots\},t)\ .\end{aligned}\tag{A1}$$

The transition probabilities W_{nm} and U_n satisfy the detailed balance condition. In the present paper, we adopt the following expressions for the transition probabilities which satisfy the detailed balance condition:

$$W_{nm}(\rho_n\to\rho_n+\Delta;\rho_m\to\rho_m-\Delta)=(a_{nm}/\Delta^2)\exp\left[-\frac{\beta}{2}[\Phi(\{\ldots,\rho_n+\Delta,\ldots,\rho_m-\Delta,\ldots\})-\Phi(\{\ldots,\rho_n,\ldots,\rho_m,\ldots\})]\right],\tag{A2}$$

$$U_n(\rho_n\to\rho_n+\Delta)=(b_n/\Delta^2)\exp\left[-\frac{\beta}{2}[\Phi(\{\ldots,\rho_n+\Delta,\ldots\})-\Phi(\{\ldots,\rho_n,\ldots\})]\right],\tag{A3}$$

where Φ is the free energy of the system and $\beta=1/k_BT$. Coefficients a_{nm} and b_n are symmetric in the configurations $\{\rho_l\}$ before and after the transition.

We shall assume that Δ is small and the distribution function $P(\{\rho_l\},t)$ and free energy Φ are slowly varying functions of $\{\rho_l\}$ within the interval of size Δ. Thus, we can expand the rhs of Eq. (A1) in powers of Δ. Keeping only the terms which are finite in the limit of $\Delta\to0$, we obtain the following equation for $P(\{\rho_l\},t)$:[19]

$$\begin{aligned}\frac{\partial}{\partial t}P(\{\rho_l\})=&\sum_{(n,m)}A_{nm}(\beta)\left[\beta\left[\frac{\partial^2\Phi}{\partial\rho_n^2}-2\frac{\partial^2\Phi}{\partial\rho_n\,\partial\rho_m}+\frac{\partial^2\Phi}{\partial\rho_m^2}\right]+\beta\left[\frac{\partial\Phi}{\partial\rho_n}-\frac{\partial\Phi}{\partial\rho_m}\right]\left[\frac{\partial}{\partial\rho_n}-\frac{\partial}{\partial\rho_m}\right]\right.\\&\left.+\left[\frac{\partial^2}{\partial\rho_n^2}-2\frac{\partial^2}{\partial\rho_n\,\partial\rho_m}+\frac{\partial^2}{\partial\rho_m^2}\right]\right]P(\{\rho_l\})\\&+\sum_{n}B_n(\beta)\left[\beta\frac{\partial^2\Phi}{\partial\rho_n^2}+\beta\frac{\partial\Phi}{\partial\rho_n}\frac{\partial}{\partial\rho_n}+\frac{\partial^2}{\partial\rho_n^2}\right]P(\{\rho_l\})\ .\end{aligned}\tag{A4}$$

Here, we have assumed that a_{nm} and b_n as functions of Δ are sharply peaked in the vicinity of $\Delta=0$, and performed the summation over Δ in the rhs of Eq. (A1) over a_{nm} and b_n. This yields the following expressions for A_{nm} and B_n in Eq. (A4):

$$\begin{aligned}A_{nm}(\beta)&=\tfrac{1}{2}\sum_{\Delta}a_{nm}(\Delta,\beta)\ ,\\B_n(\beta)&=\tfrac{1}{2}\sum_{\Delta}b_n(\Delta,\beta)\ .\end{aligned}\tag{A5}$$

Equation (A4) can easily be transformed into a more familiar form of the Fokker-Planck equation if we introduce dimensionless free energy $\tilde{\Phi}=\beta\Phi$ and take into account the fact that A_{nm} is symmetric with respect to the interchange of the subscripts n and m,

$$\frac{\partial}{\partial t}P(\{\rho_l\})=\sum_{n,m}\Delta_{nm}\frac{\partial}{\partial\rho_n}\left[\frac{\partial\tilde{\Phi}}{\partial\rho_m}+\frac{\partial}{\partial\rho_m}\right]P(\{\rho_l\})\ ,\tag{A6}$$

where Δ_{nm} represents the kinetic coefficients given by

$$\Delta_{nm}=\begin{cases}\sum_{l(\neq n)} A_{nl}(\beta)+B_n(\beta), & n=m \\ -A_{nm}(\beta), & n\neq m\ .\end{cases} \tag{A7}$$

In the present paper, we assume that the exchange process, i.e., diffusion process, takes place only between nearest-neighbor cells so that matrix elements of A_{nm} are nonzero only between $n=m\pm1$. Besides, we neglect the temperature dependence of the matrix elements of A_{nm} and B_n and take them as constant,

$$\begin{aligned}&A_{nm}(\beta)=\begin{cases}A, & n=m\pm1\\ 0, & \text{otherwise}\end{cases}\\ &B_n(\beta)=B\ .\end{aligned} \tag{A8}$$

Substitution of Eq. (A8) into Eq. (A7) yields the following expression for Δ_{nm}:

$$\Delta_{nm}=\begin{cases}zA+B, \\ -A\ ,\end{cases} \tag{A9}$$

where z is the coordination number of cells which is equal to two in the present single-column model.

It is straightforward to derive the Langevin equation which is equivalent to the Fokker-Planck equation (A6).[20] Suppose we have the following Langevin equation:

$$\frac{d}{dt}\rho_n=F_n(\{\rho_l\})+\sum_m G_{nm}\xi_m(t)\quad (n=1,2,\ldots,p)\ , \tag{A10}$$

where $\{\xi_n(t)\}$ are independent, Gaussian and δ correlated random forces with zero mean and unit intensities

$$\begin{aligned}&\langle\xi_m(t)\rangle=0\ ,\\ &\langle\xi_m(t)\xi_n(t')\rangle=\delta_{nm}\delta(t-t')\ .\end{aligned} \tag{A11}$$

Then, the expressions for F_n and G_{nm} are given in terms of Δ_{nm} and Φ by

$$F_n(\{\rho_l\})=-\sum_m \Delta_{nm}\beta\frac{\partial\Phi}{\partial\rho_m}\ , \tag{A12}$$

$$\sum_l G_{nl}G_{lm}=2\Delta_{nm}\ , \tag{A13}$$

if we assume that Δ_{nm} is independent of $\{\rho_l\}$. Substitution of Eq. (A12) into Eq. (A10) yields the systematic term in the rhs of the Langevin equation (2.4).

Equations (A10) and (A13) suggest that we can conveniently introduce a new set of random forces instead of $\xi_n(t)$ defined by

$$f_n(t)=\sum_m G_{nm}\xi_m(t)\ . \tag{A14}$$

As is shown from Eqs. (A11) and (A13), this set of random forces satisfy the following relations:

$$\begin{aligned}&\langle f_m(t)\rangle=0\ ,\\ &\langle f_m(t)f_n(t')\rangle=2\Delta_{nm}\delta(t-t')\ .\end{aligned} \tag{A15}$$

This completes the derivation of the Langevin equation (2.4).

[1]For an overview, see R. Clarke and C. Uher, Adv. Phys. **33**, 469 (1984).

[2]N. Daumas and C. Hérold, C. R. Acad. Sci., Ser. C **268**, 273 (1969).

[3]S. A. Safran, Synth. Met. **2**, 1 (1980).

[4]P. Hawrylak and K. R. Subbaswamy, Phys. Rev. Lett. **53**, 2098 (1984).

[5]G. Kirczenow, Phys. Rev. Lett. **52**, 437 (1984).

[6]M. E. Misenheimer and H. Zabel, Phys. Rev. Lett. **54**, 2521 (1985).

[7]R. Nishitani, Y. Uno, and H. Suematsu, Phys. Rev. B **27**, 6572 (1983).

[8]M. E. Misenheimer and H. Zabel, Phys. Rev. B **27**, 1443 (1983).

[9]S. A. Safran, Phys. Rev. Lett. **44**, 937 (1980).

[10]S. Ohnishi and S. Sugano, Solid State Commun. **36**, 823 (1980).

[11]S. A. Safran and D. R. Hamman, Phys. Rev. Lett. **42**, 1410 (1979).

[12]L. Pietronero, S. Strassler, H. R. Zeller, and M. J. Rice, Phys. Rev. Lett. **41**, 763 (1978).

[13]S. E. Millman and G. Kirczenow, Phys. Rev. B **26**, 2310 (1982).

[14]S. A. Safran and D. R. Hamman, Phys. Rev. B **22**, 606 (1981).

[15]R. Petschek and H. Metiu, J. Chem. Phys. **79**, 3443 (1983).

[16]P. Bak and G. Forgacs, Phys. Rev. B **32**, 7535 (1985).

[17]G. Kirczenow, Phys. Rev. Lett. **55**, 2810 (1985).

[18]C. C. Shieh, R. L. Schmidt, and J. E. Fischer, Phys. Rev. B **20**, 3351 (1979); K. Suda and H. Suematsu (private communication).

[19]J. S. Langer, Ann. Phys. (Paris) **65**, 53 (1971).

[20]R. L. Stratonovich, *Topics in the Theory of Random Noise* (Gordon and Breach, New York, 1981), Vol. 1, p. 100.